

SUPPLEMENTAL MATERIAL

Injectable Shear-Thinning Hydrogels for Minimally Invasive Delivery to Infarcted Myocardium to Limit Left-Ventricular Remodeling

Christopher B. Rodell, PhD,¹ Madonna E. Lee, MD,² Hua Wang,³ Satoshi Takebayashi, MD,² Tetsushi Takayama, MD,² Tomonori Kawamura, MD,² Jeffrey S. Arkles, MD,² Neville N. Dusaj,¹ Shauna M. Dorsey, PhD,¹ Walter R.T. Witschey, PhD,⁴ James J. Pilla, PhD,⁴ Joseph H. Gorman, III, MD,² Jonathan F. Wenk, PhD,^{3,5} Jason A. Burdick, PhD,^{1,*} Robert C. Gorman, MD^{2,*}

¹ Department of Bioengineering, University of Pennsylvania, Philadelphia, Pennsylvania 19104

² Gorman Cardiovascular Research Group, Department of Surgery, University of Pennsylvania, Philadelphia, Pennsylvania 19104

³ Department of Mechanical Engineering, University of Kentucky, Lexington, Kentucky 40506

⁴ Department of Radiology, University of Pennsylvania, Philadelphia, Pennsylvania 19104

⁵ Department of Surgery, University of Kentucky, Lexington, Kentucky 40506

*Corresponding Authors

SUPPLEMENTAL METHODS

Polymer Synthesis.

Sodium hyaluronic acid (HA, 90kDa) was purchased from Lifecore (Chaska, MN). β -cyclodextrin (CD) and 1-adamantane acetic acid (Ad) were purchased from TCI America. All other reagents were purchased from Sigma, unless otherwise indicated. Following modification, modified hyaluronate was purified by dialysis (and vacuum filtration, where necessary to remove insoluble impurities) and recovered by lyophilization. Polymer modifications were determined by ^1H NMR acquired at 360MHz (Bruker). Disaccharide modifications were approximately 25% of repeat groups; Ad-HA utilized in percutaneous delivery had a 50% modification.

HA-TBA and MeHA-TBA: To enable anhydrous reactions in DMSO, the tetrabutylammonium (TBA) salt of HA was prepared. The sodium salt of HA or methacrylated HA (MeHA; synthesized by the typical esterification with methacrylic anhydride¹) was dissolved in DI water at 2.0 wt%, exchanged against Dowex-100 resin, neutralized by tetrabutylammonium hydroxide, and lyophilized.

Ad-HA Synthesis: Ad-HA was prepared by esterification of HA-TBA with Ad via BOC_2O /DMAP catalysis. A round bottom flask was charged with HA-TBA (1 eq), Ad (3 eq), and 4-dimethylaminopyridine (DMAP; 1.5 eq). Anhydrous DMSO was added via cannulation under nitrogen, affording a 2 wt% solution. Di-tert-butyl dicarbonate (BOC_2O) was added (0.5 eq) and the reaction allowed to proceed at 45°C overnight.

CD-HA and CD-MeHA Synthesis. CD-HA was prepared by coupling 6-(6-aminohexyl)amino-6-deoxy- β -cyclodextrin (β -CD-HDA) to HA-TBA via amidation. A round bottom flask was charged with HA-TBA (1 eq) and β -CD-HDA (0.5 eq). Anhydrous DMSO was added via cannulation under nitrogen, affording a 2 wt% solution. Once dissolved, (benzotriazol-1-yloxy)tris(dimethylamino)phosphonium hexafluorophosphate (BOP; 0.5 eq) was dissolved in minimal DMSO and transferred to the reaction vessel via cannulation. The reaction was allowed to proceed at room temperature for >2 hours. CD-MeHA was identically prepared, with MeHA-TBA as the starting material.

Ad-HA-SH Synthesis. Ad-HA-SH was prepared by modifying HA with Ad and subsequent thiolation. A portion of Ad-HA was converted to the TBA salt as described above. Esterification of Ad-HA-TBA with 3,3'-dithiopropionic acid (5.0 eq) was performed (2.50 eq DMAP, 1.0 eq BOC_2O) similarly to Ad-HA modification. Following purification, the disulfide was reduced by DTT.

MRI Acquisition Parameters.

T_2 weighted turbo spin echo: matrix size = 320 x 256 x 65, voxel size = 0.3125 x 0.3125 x 1.0 mm³, repetition time = 1128 ms, echo time = 71 ms, 4 signal averages.

TrueFISP CINE: field of view = 280x166.25 mm, acquisition matrix = 256 x 152 pixels, repetition time = 27.52 ms, echo time = 1.46 ms, BW = 930 Hz/pixel, slice thickness = 4 mm.

LGE spoiled gradient echo sequence: field of view = 218 x 350, acquisition matrix = 256 x 160, repetition time = 5.50 ms, echo time = 2.42 ms, BW 244 Hz/pixel, slice thickness = 4 mm, 2 signal averages. Acquisition was performed approximately 15 minutes following bolus intravenous injection of 0.1 mmol/kg gadobenate dimeglumine (MultiHance; Bracco Diagnostics, Inc.).

MRI Analysis.

Examination of hydrogel distribution in explanted tissue was performed by 3D reconstruction of the hydrogel and myocardial segments (ITK-Snap²). Longitudinal analysis of infarct thickness was performed from CINE MRI. Three consecutive short axis images were isolated at end-diastole from the infarcted region, immediately sub-papillary where possible. The infarct was confirmed from corresponding LGE images, and the location was maintained across all time points. For each image, 5 radial lines were drawn from epicardium to endocardium and measured (ImageJ; **Fig. S3**) and reported values represent the average of all 15 measurements for each animal. Analyses were repeated in the remote region along the contralateral LV wall.

Toward assessment of LV dilation and function, volumetric analysis was performed. CINE images were sorted and cropped using customized programming (MATLAB). Through all acquired planes and phases, semi-automated segmentation of the intraventricular space was performed with manual correction as necessary (ITK-Snap). Repartitioning of the images into the time-space and corresponding volumetric reconstruction enabled determination of the LV volume as a function of time, from which the minimum volume (LVESV), maximum volume (LVEDV), SV, and EF were determined.

Finite Element (FE) Modeling.

Myocardial Dimensions. To evaluate the effects of hydrogel injections on myocardial wall stress, finite element (FE) models of the LV were generated. The geometry of the LV wall was based on measurements at end-systole in ovine hearts; images were acquired via TrueFISP CINE sequences. The wall thickness was 1.3 cm, the inner diameter of the endocardial wall near the equator was 4.0 cm, and the distance from base to apex was 6.4 cm. To simulate hydrogel injection, the base model was modified to include 16 injections in a 4-by-4 array within the free wall (**Fig. S1**). The size and shape of the hydrogel injections were based on MR images of injected explant tissue (**Fig. S2, Table S1**), where the injections were approximated as ellipsoids where the volume is given by the equation:

$$V = \frac{4}{3}\pi(a * b * c) \quad (1)$$

The spacing between injections was determined to be 1.5 cm from center-to-center, based on expected anatomical measures. Each injection was 0.3 mL, resulting in a total volume of 4.8 mL added to the model. To account for volumetric addition, the myocardial wall thickness throughout the injection regions was increased to 1.5 mm, thus preserving the total volume of myocardium (**Fig. S1B**). The longitudinal dimensions were unaltered, as were dimensions in remote regions, away from the injection site.

Material Properties and Loading Conditions. The material response of the myocardium was represented using a nearly incompressible, transversely isotropic, hyperelastic constitutive law, which was defined using the strain energy function:

$$W_{myocardium} = \frac{C}{2} \left(e^{b_f E_{ff}^2 + b_t (E_{ss}^2 + E_{nn}^2 + E_{ns}^2 + E_{sn}^2) + b_{fs} (E_{fs}^2 + E_{sf}^2 + E_{fn}^2 + E_{nf}^2)} - 1 \right) + \frac{\kappa}{2} (J - 1)^2 \quad (2)$$

where E_{ij} are the deviatoric components of the Green-Lagrange strain tensor relative to the myofiber coordinate system (f = fiber direction, s = cross-fiber in-plane direction, n = transverse-fiber direction) and J is the determinant of the deformation gradient. The diastolic material parameters were assigned to be $C = 0.51$ kPa, $b_f = 22.84$, $b_t = 3.45$, and $b_{fs} = 12$, while the bulk modulus was $\kappa = 1 \times 10^3$ kPa.³ Since the model was intended to mimic the initial time frame after infarction, it was assumed that the properties would be unchanged during this timeframe.⁴ Hence, the model was created such that the myocardial material properties around the hydrogel injections were the same as in remote regions. The myofiber orientation was assigned to vary linearly from epicardium to endocardium using the angles of -37 degrees to 83 degrees,

respectively. The material response of the hydrogel injections was represented using a nearly incompressible, isotropic, hyperelastic constitutive law, which was defined using the strain energy function:

$$W_{injection} = \frac{E}{2(1+\nu)} \text{tr}(\mathbf{E}^2) + \frac{E}{6(1-2\nu)} \ln(J)^2 \quad (3)$$

where \mathbf{E} is the deviatoric Green-Lagrange strain tensor, $\text{tr}(\)$ is the trace operator, and $\ln(\)$ is the natural log operator. The material parameters for Young's modulus (E) were assigned based on the experimental measurements of the GH and DC hydrogels, while the Poisson ratio (ν) was assigned a value of 0.499. A pressure of 10 mmHg was assigned as a boundary condition on the endocardial wall in each of the FE models, simulating end-diastolic loading conditions. For all data presented, the results depict the mean \pm standard deviation (SD) of the path length or myofiber stress of adjacent elements ($n \geq 6$) along the path indicated.

SUPPLEMENTAL TABLES

Table S1. Ellipsoid dimensions of a 0.3 mL hydrogel injection, based on MRI data.

| | |
|---|--------|
| a | 6.60mm |
| b | 3.94mm |
| c | 2.73mm |

Table S2. Animal usage and assessment of gross cardiac geometry.

| Category/ Metric | MI | GH | DC |
|---------------------------------------|--------------------|--------------------|--------------------|
| Animal Usage | | | |
| Number Included | 7 | 7 | 6 |
| Weight (kg), Baseline | 39.7 \pm 1.1 | 44.4 \pm 1.8 | 43.7 \pm 2.0 |
| Weight (kg), 2 WK | 38.9 \pm 0.8 | 42.0 \pm 2.3 | 43.0 \pm 1.9 |
| Weight (kg), 8 WK | 46.6 \pm 1.0 | 51.4 \pm 1.7 | 51.3 \pm 1.3 |
| Heart Size, 8 WK | | | |
| Heart Mass (g) | 274.99 \pm 16.20 | 306.42 \pm 13.53 | 300.63 \pm 18.43 |
| RV Mass (g) | 71.03 \pm 14.01 | 58.20 \pm 3.59 | 62.18 \pm 4.64 |
| LV Mass (g) | 141.00 \pm 18.78 | 166.84 \pm 4.02 | 169.88 \pm 9.02 |
| Infarct Geometry | | | |
| Initial Infarct Area (% LV) | 19.4 \pm 0.6 | 18.6 \pm 0.7 | 19.3 \pm 0.7 |
| Final LV Area (cm ²) | 19.35 \pm 0.78 | 18.36 \pm 1.22 | 17.25 \pm 1.34 |
| Final Infarct Area (cm ²) | 98.56 \pm 5.96 | 98.85 \pm 3.85 | 103.58 \pm 4.41 |
| Final Infarct Size (% LV) | 19.31 \pm 1.97 | 18.15 \pm 1.43 | 17.93 \pm 1.81 |

Data provided as mean \pm SEM.

No differences observed between groups ($P > 0.05$ by ANOVA).

Table S3. Direct measurement of myocardial thickness at 8 weeks post-MI.

| Treatment Group/ Region | Base Thickness (mm) | Infarct Thickness (mm) | Apical Thickness (mm) |
|----------------------------|------------------------|---------------------------|--------------------------|
| MI | | | |
| Infarcted Region | 11.11 ± 0.96 | 3.90 ± 0.48 | 8.49 ± 1.08 |
| Remote Region | 13.31 ± 1.04 | 12.39 ± 1.13 | 10.51 ± 0.49 |
| GH | | | |
| Infarcted Region | 11.25 ± 0.27 | 5.79 ± 0.96 | 8.66 ± 0.42 |
| Remote Region | 12.38 ± 0.85 | 11.13 ± 0.50 | 9.69 ± 0.74 |
| DC | | | |
| Infarcted Region | 11.92 ± 0.20 | 9.92 ± 0.24* [#] | 9.08 ± 0.84 |
| Remote Region | 11.75 ± 0.21 | 11.10 ± 0.25 | 9.82 ± 0.32 |

Data provided as mean±SEM.

* P < 0.05 relative to MI

[#] P < 0.05 relative to GH

Table S4. MRI assessment of myocardial thickness over time.

| Treatment Group/ Timepoint | Infarct Thickness (mm) | Remote Thickness (mm) |
|-------------------------------|----------------------------|--------------------------|
| MI | | |
| Baseline | 9.44 ± 0.14 | 9.81 ± 0.28 |
| 2 Weeks | 4.39 ± 0.43 | 9.94 ± 0.34 |
| 8 Weeks | 3.56 ± 0.19 | 10.31 ± 0.22 |
| GH | | |
| Baseline | 8.92 ± 0.24 | 9.32 ± 0.18 |
| 2 Weeks | 6.98 ± 0.46* | 9.76 ± 0.40 |
| 8 Weeks | 5.51 ± 0.23* | 9.70 ± 0.22 |
| DC | | |
| Baseline | 10.90 ± 0.44* [#] | 10.79 ± 0.48 |
| 2 Weeks | 11.39 ± 1.16* [#] | 10.78 ± 0.31 |
| 8 Weeks | 10.02 ± 0.79* [#] | 11.21 ± 0.41* |

Data provided as mean±SEM.

* P < 0.05 relative to MI

[#] P < 0.05 relative to GH

SUPPLEMENTAL FIGURES

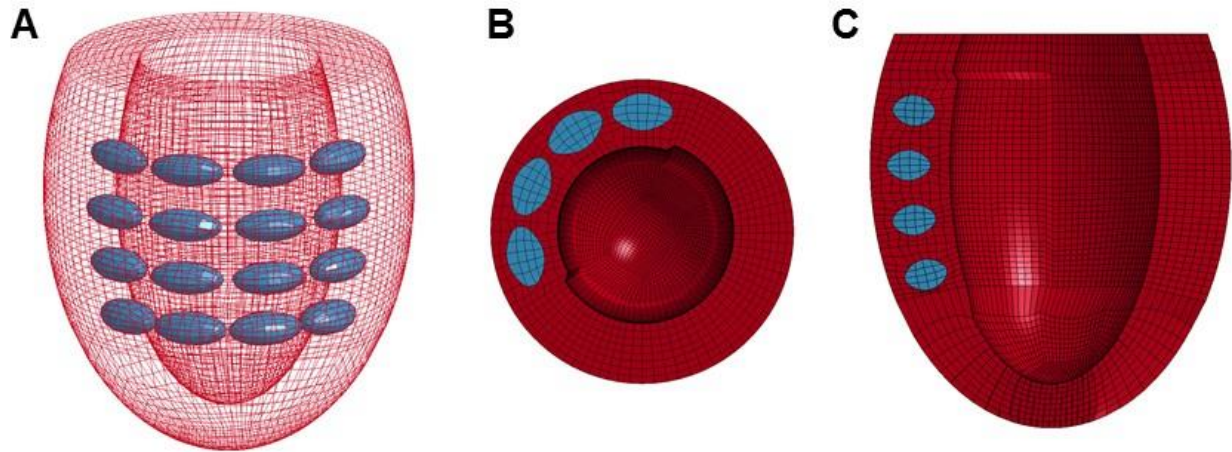


Figure S1. (A) Finite element model of ovine LV with 16 hydrogel injections in the free wall. The injections were modeled as ellipsoids, which caused the LV wall to thicken. (B) Short axis view of LV wall. (C) Long axis view of LV wall.

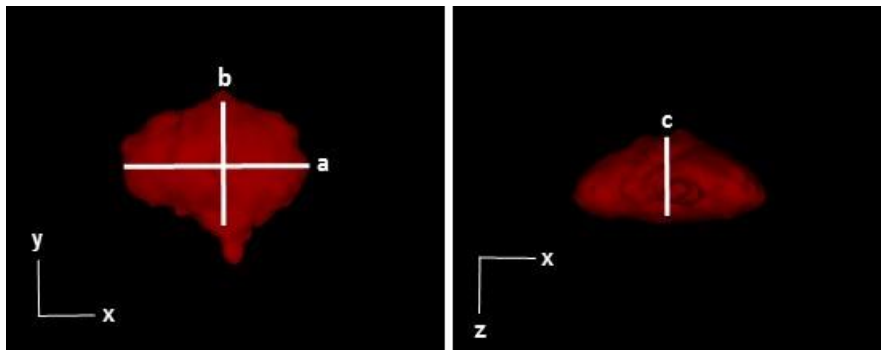


Figure S2. Reconstruction of hydrogel geometry based on MRI data of injections embedded in myocardial wall. Note that the shape is approximately ellipsoidal and a volume of 0.298mL was directly determined from the reconstruction in ITK-Snap.

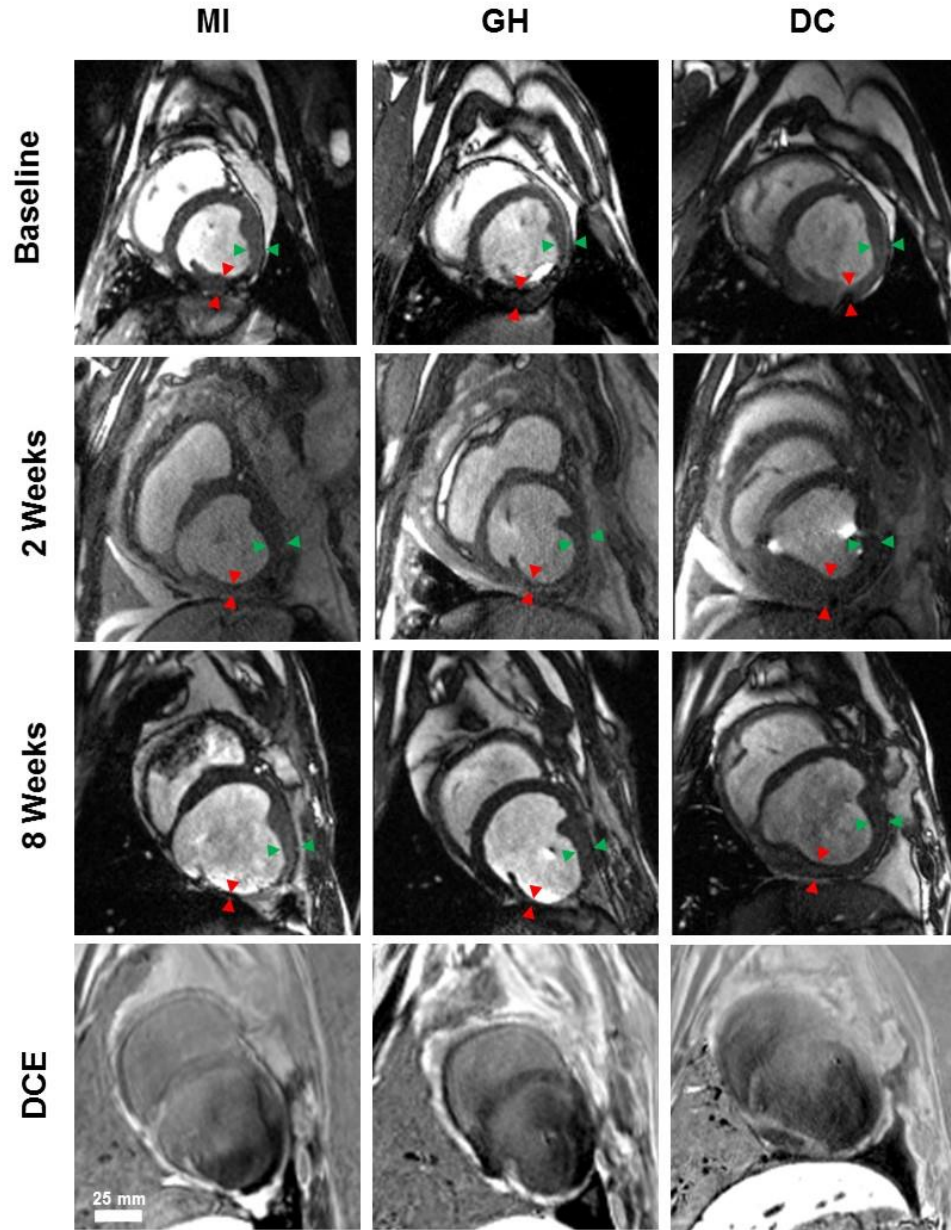


Figure S3. MRI based determination of myocardial thickness over time. Red and green arrows indicate infarct and remote thickness, respectively, as assessed for MI (left), GH (middle), and DC (right) treatment groups. Measurements were performed (3 slices, n = 5 measurements per slice) at baseline, 2 weeks, and 8 weeks, with delayed contrast enhancement (DCE) used to confirm measurements were made within the infarcted region (myocardial wall in white contrast).

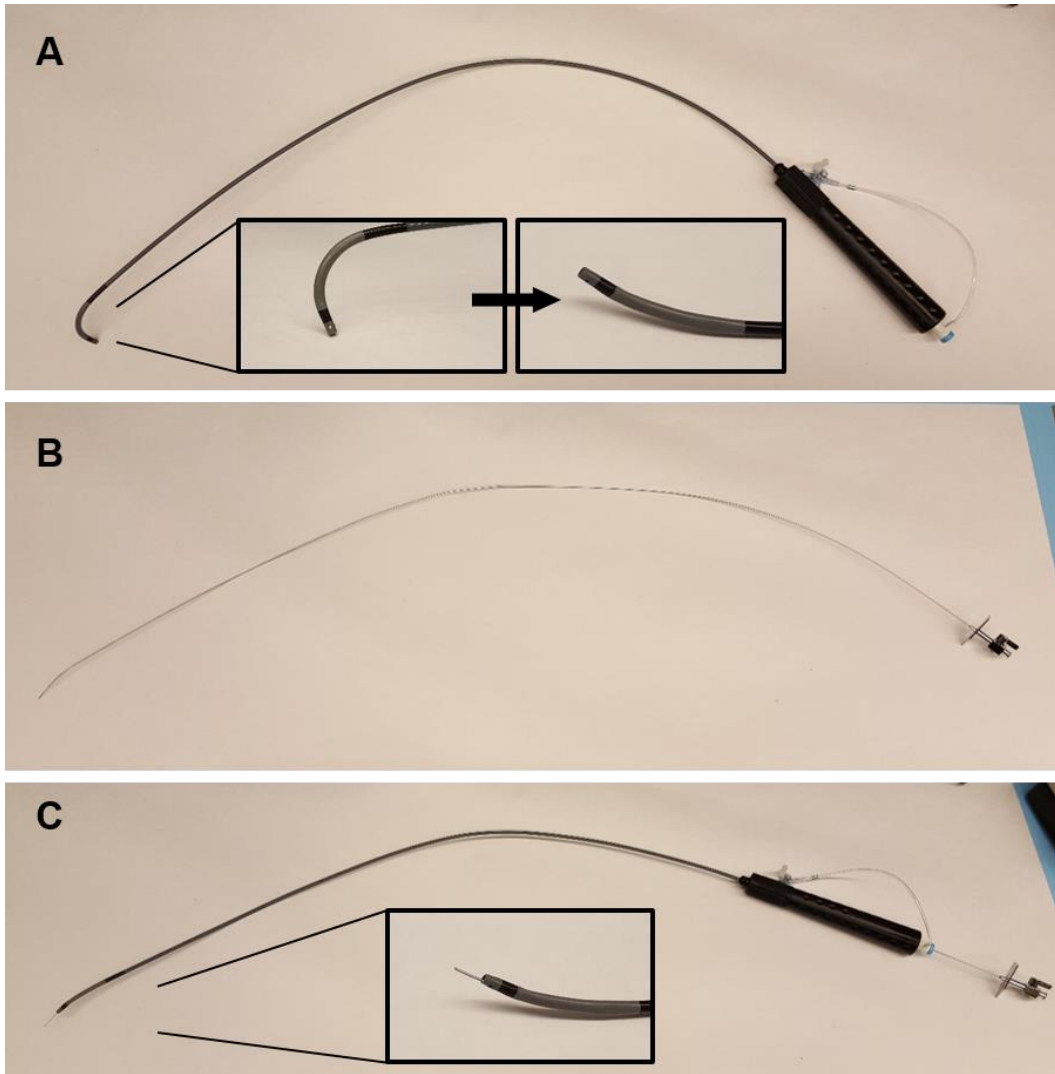


Figure S4. Hydrogel delivery system. The Agilis™ NxT steerable introducer (A) allowed for user-controlled deflection of needle tip (inset) to guide injection location. A BRK™ transseptal needle (B, 4 Fr, 90 cm; St. Jude Medical) was used for injection by insertion through the introducer (C), where injection depth was controlled by the length of needle deployment (inset).

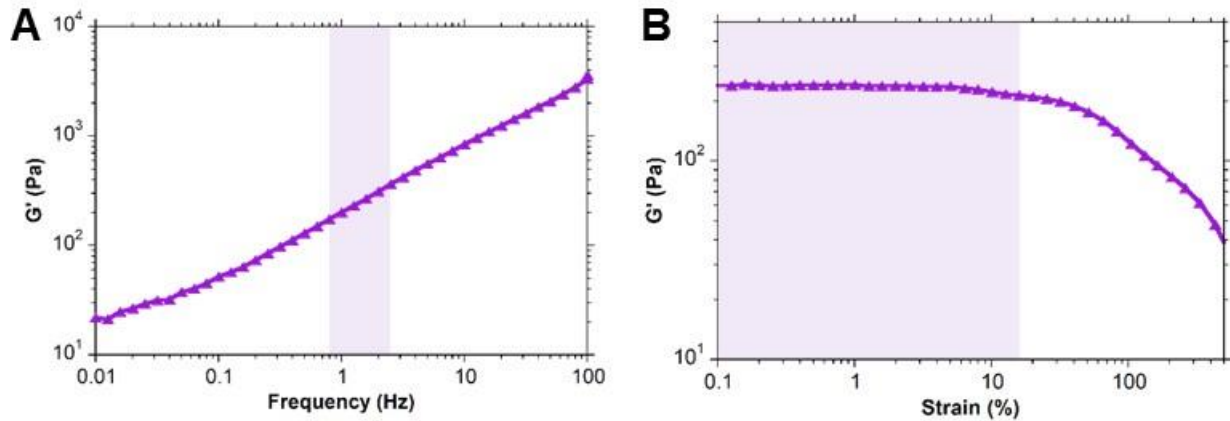


Figure S5. (A) Frequency sweep (1.0 % strain, 37°C) showing frequency dependence of GH hydrogel shear moduli (G'). Relevant moduli were estimated at 1.6 Hz, corresponding to a heart rate of approximately 100 BPM. Elastic moduli (E) estimated assuming an incompressible solid whereby $E = 3 \cdot G'$. (B) Strain sweep (1.0 Hz, 37°C) showing strain dependence of GH hydrogel shear moduli (G'). Shear-induced loss of GH mechanics and corresponding flow is not observed below strains of ~40%. Approximate physiological range (maximum strain of 10-15%)^{5,6} is indicated (shaded regions).

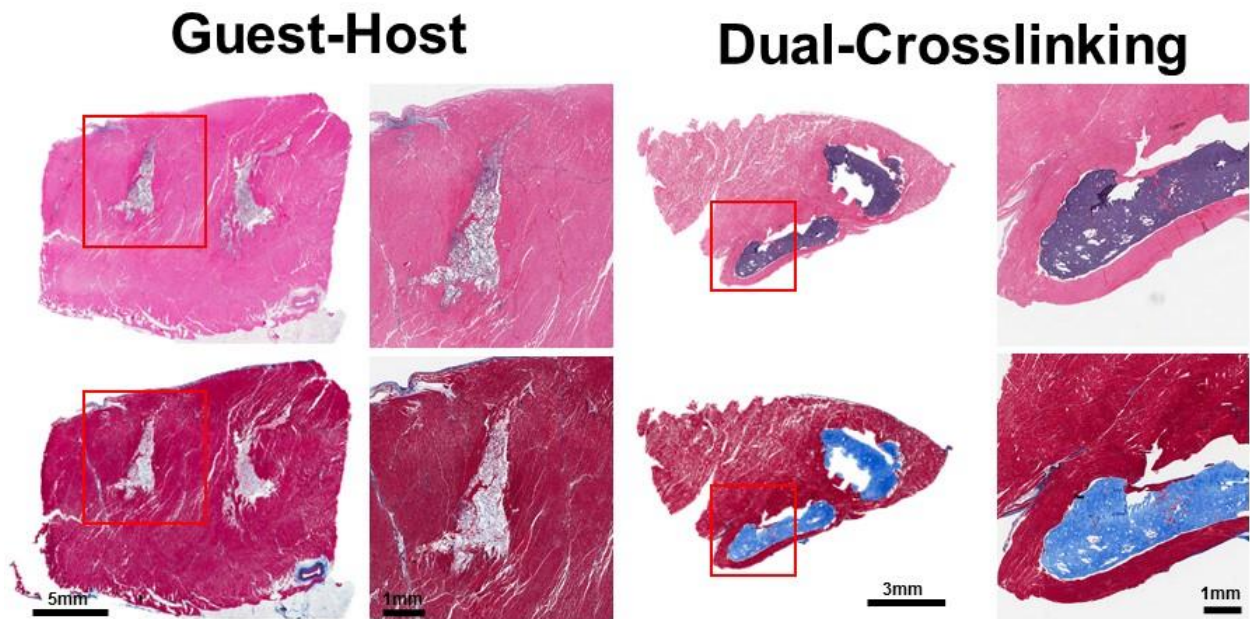
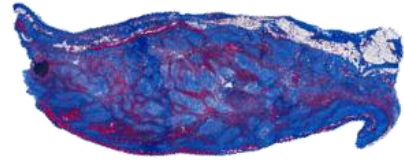
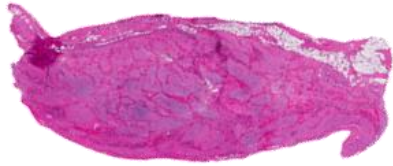
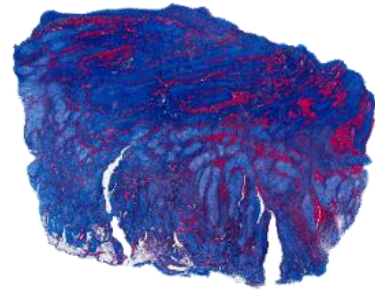


Figure S6. Representative histological examination of guest-host (GH) and dual-crosslinking (DC) injections within the infarct region at 24 hours post-injection by H&E (top) and trichrome (bottom) with the expanded region indicated.

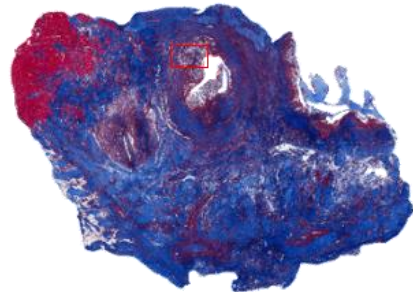
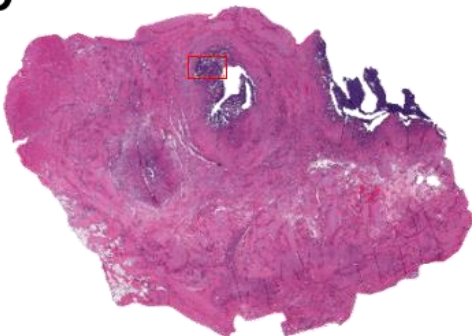
MI



GH



DC



Remote



Figure S7. Low magnification histological examination 8 weeks post-MI of myocardial tissue from the infarct region in control (MI), guest-host (GH), and dual-crosslinking (DC) groups with remote section provided for reference. H&E (left) and trichrome (right), with the expanded region (provided in Figure S8) indicated for DC injection.

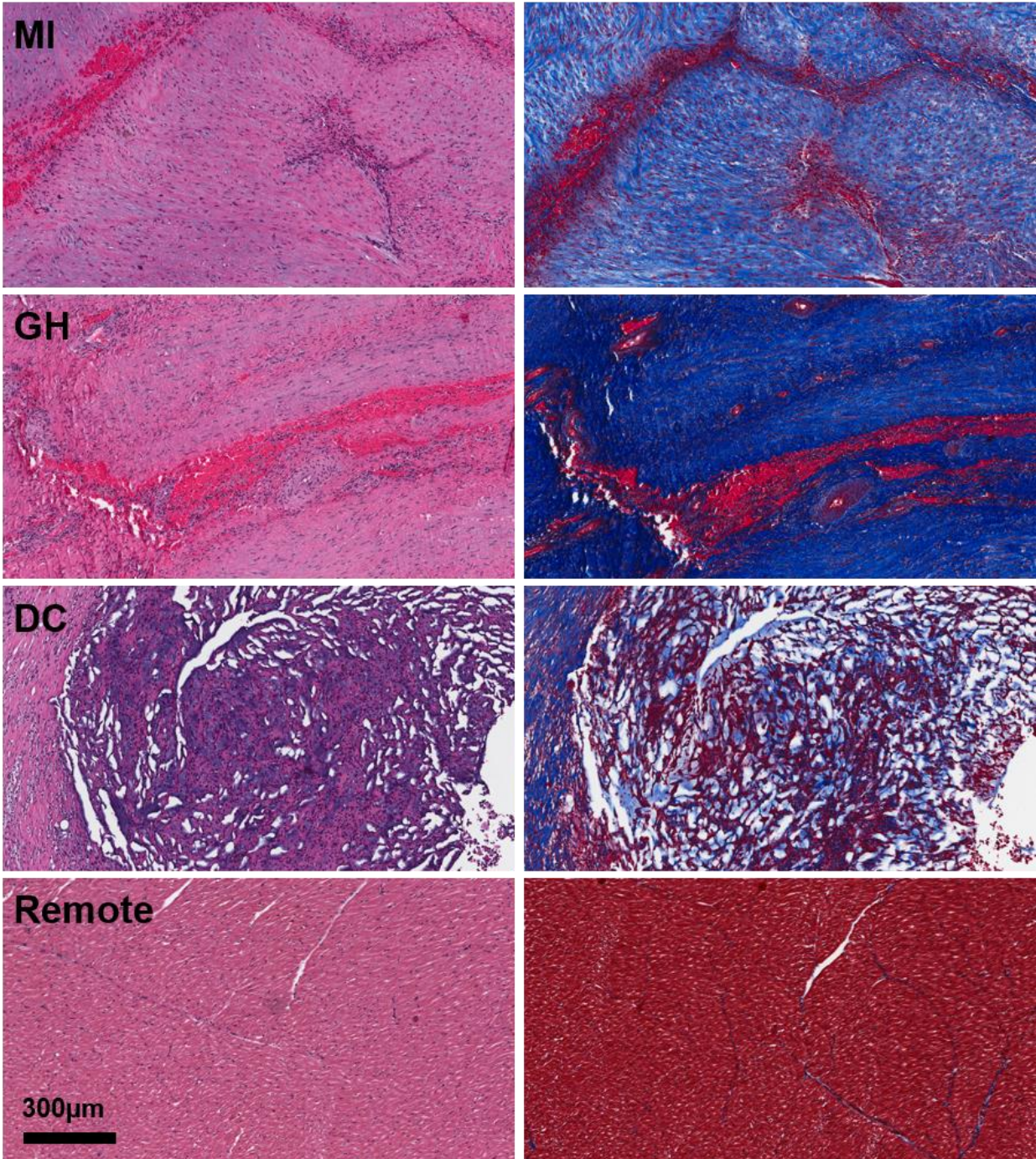


Figure S8. High magnification histological examination 8 weeks post-MI of myocardial tissue from the infarct region in control (MI), guest-host (GH), and dual-crosslinking (DC) groups with remote section provided for reference. H&E (left) and trichrome (right), where DC hydrogel visible by H&E staining (dark purple) and trichrome (light blue) integrated with viable tissue. Other groups demonstrate fibrosis (trichrome, dark blue) without indication of remaining hydrogel.

SUPPLEMENTAL REFERENCES

1. Smeds KA, Grinstaff MW. Photocrosslinkable polysaccharides for in situ hydrogel formation. *J. Biomed. Mater. Res.* 2001;54:115-121
2. Yushkevich PA, Piven J, Hazlett HC, Smith RG, Ho S, Gee JC, Gerig G. User-guided 3d active contour segmentation of anatomical structures: Significantly improved efficiency and reliability. *Neuroimage.* 2006;31:1116-1128
3. Kichula ET, Wang H, Dorsey SM, Szczesny SE, Elliott DM, Burdick JA, Wenk JF. Experimental and computational investigation of altered mechanical properties in myocardium after hydrogel injection. *Ann Biomed Eng.* 2014;7:1546-1556
4. Holmes JW, Borg TK, Covell JW. Structure and mechanics of healing myocardial infarcts. *Annual review of biomedical engineering.* 2005:223-253.
5. Chuong CJ, Sacks MS, Templeton G, Schwiep F, Johnson RL. Regional deformation and contractile function in canine right ventricular free wall. *Am. J. Physiol.* 1991;260:H1224-H1235
6. Rappaport D, Adam D, Lysyansky P, Riesner S. Assessment of myocardial regional strain and strain rate by tissue tracking in b-mode echocardiograms. *Ultrasound Med. Biol.* 2006;32:1181-1192